NOISE-TOLERANT RANGE ANALYSIS FOR AUTONOMOUS NAVIGATION *

Aviv Bergman and Cregg K. Cowan

Robotics Laboratory, SRI International
333 Ravenswood Avenue, Menlo Park, California 94025

ABSTRACT

Techniques for detecting horizontal regions, obstacles, ditches, and shoulders along a road from range data are described. The noise level in each scan line of the range image is computed and an adaptive threshold is used for noise compensation. The sources of noise and the scanning geometry for a time-of-flight range sensor are discussed and experimental results of applying these techniques to ERIM range images are presented.

I INTRODUCTION

Autonomous navigation in an outdoor environment requires solutions to such problems as finding the road or other route, detecting and avoiding obstacles, and distinguishing between true obstacles, such as boulders, and apparent obstacles, such as shrubs.

This paper presents some techniques for analyzing range images of road scenes. Assuming the vehicle is on a road (a region that is horizontal relative to the vehicle), these techniques measure the noise characteristics of the range image and use this information to find the boundaries of the road region, identify obstacles in the road, and locate ditches and shoulders along the road.

In Section II we describe the range sensing technique, the sensor geometry, and sources of noise in range images. In Section III we describe and illustrate the techniques for measuring the noise level, detecting the horizontal region boundary, finding obstacles, and locating ditches and shoulders along the road.

* The research reported herein was supported by the FMC Corporation, Ordnance Division, San Jose, California, under P.O. 147466, Work Directive 014.

II DESCRIPTION OF RANGE IMAGERY

In this section we describe characteristics of range sensors that use the phase difference between the reference and reflected signals of a modulated laser beam to determine the range to a surface [1]. See [3] and [4] for a detailed description of this method. Figure 1 contains a typical road scene and corresponding range image detected by a sensor from the Environmental Research Institute of Michigan (ERIM). These images were obtained from the Martin Marietta Corporation.

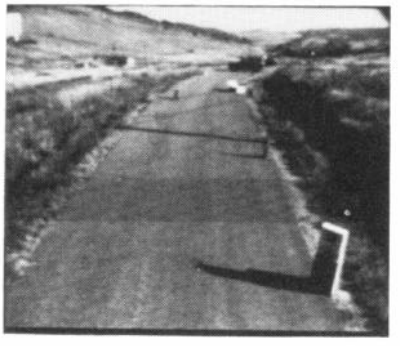

a. Road scene

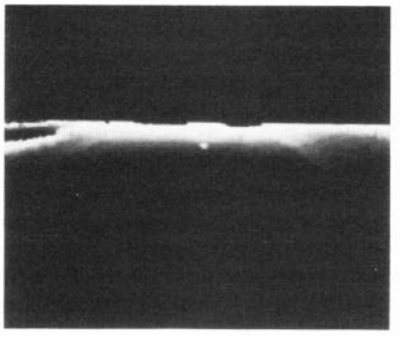

b. Range image (distance encoded as intensity)

Figure 1: Typical Road Scene and Range Image

Because the ERIM sensor uses the phase difference between two signals to measure distance, the range values obtained are inherently ambiguous--objects whose distance from the sensor differs by exactly one modulation cycle have the same range value. For the ERIM sensor, the distance corresponding to one modulation cycle (the ambiguity interval) is 64 feet.

A. Scanning Geometry

The configuration for sensing the range **r** to a world point **P** is illustrated in Figure 2. In this diagram the sensor lies on the z axis with its principal ray in the x-z plane. The tilt of the sensor is given by angle ψ, and β is the pan angle from the center of the scan line. An ERIM range image consists of 64 horizontal scan lines, and each scan line contains 256 range values (obtained by sweeping the laser from $-\beta_{max}$ to $+\beta_{max}$).

B. Sources of Noise in Range Images

Two noise effects of particular interest for an autonomous vehicle operating in an outdoor environment are absorption and scattering of the laser beam by the atmosphere and noise contributed by background radiation, such as sunlight. Other noise sources for a laser ranging device are described in [5].

The transmission loss from atmospheric effects is dependent on the range to the object surface and on the wavelength of the laser. For the ERIM sensor, the principal transmission loss is due to scattering [5] and is proportional to e^{-k2r}, where r is the range to the surface and k is a constant dependent on the laser wavelength and the visibility.

The detected signal strength also depends on the surface orientation and reflectivity. Therefore the total received signal is of the form

$$P_0 \times f\left(\frac{p\cos\theta}{r^2}\right) \times (1 - e^{-k2r})$$

where P_0 is the transmitted power, p is the diffuse surface reflectance, θ is the angle between the incident beam and the surface normal, and r is the range.

Figure 3 shows the scanning configuration for the ERIM road images. The relative angle between the road surface and the laser becomes more oblique for higher scan lines. Although the received signal decreases for higher scan lines ($\cos\theta$ decreases and r increases), the ERIM device has constant integration time for each range value, resulting in decreased signal to noise ratio for higher scan lines. (Other devices vary the integration time to achieve a constant signal to noise ratio [4]).

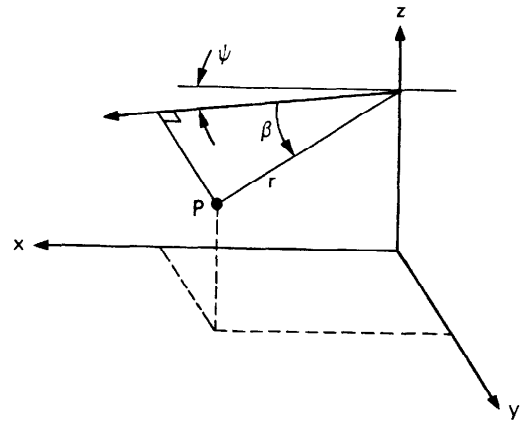

Figure 2: Sensor Geometry: Range r, Tilt ψ and Pan β

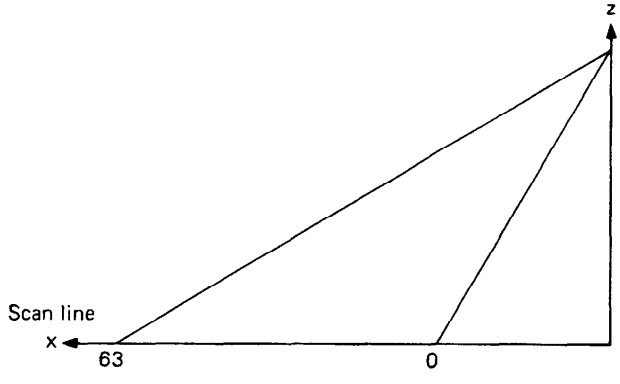

Figure 3: Configuration for Scanning a Road (Side View)

III RANGE IMAGE ANALYSIS

A. Correcting for Range Ambiguity

The first step in analyzing a range image is to remove the ambiguity interval. We analyze each column in the image starting from the bottom; if we detect a decrease in range value greater than a threshold (currently 16 feet), we assume it to be caused by the ambiguity interval and add 64 feet to the measured range value.

This simple technique fails for some cases where the laser spot spans a range discontinuity (part of the spot is on the close object and part on the more distant object). In such cases the measured range value is an average of the range to the two surfaces. If the surfaces lie in different ambiguity intervals, then the measured range value can produce an arbitrarily small decrease in range, falling below the threshold. We correct such cases by hand. A method for automatically removing the ambiguity interval is described in [2].

B. Measuring the Noise Level

Although some sources of range data noise can be modeled a priori, other noise sources, such as the orientation and reflectivity of the target surface, are not generally known. We therefore choose to estimate the total noise by measuring the statistical characteristics of the actual range data. We currently measure the mean μ and standard deviation σ for each scan line.

Consider the values for one scan line when viewing a horizontal plane (the x-y plane) that is aligned with the range sensor as shown in Figure 4a. The range sensor lies on the z axis with its principal ray in the x-z plane. The line P_1P_2 is the intersection of the x-y plane with the scanning plane (formed by sweeping from $-\beta_{max}$ to $+\beta_{max}$). The range value **r** for an arbitrary point **P** is related to the range value along the principal ray $\mathbf{r_0}$ by $[r = r_0 / \cos \beta]$. Figure 4b displays this relationship between range and pan angle.

Under the assumption that the horizontal plane is aligned with the sensor, that is, that the vehicle is not tilted relative to the road surface, the maximum range difference between the center and edge of each scan line is $(r_0 - r_0 / \cos(\beta_{max}))$. If we multiply each value by $\cos \beta$ to compensate for its pan angle, then the range values within the horizontal region become constant. Measuring the mean μ and standard deviation σ of the modified range values for each scan line can then be considered as local estimation of the noise parameters μ and σ for the range image.

Because we do not expect the horizontal region to fill the entire image, we measure μ and σ only in an "adaptive" analysis window of each scan line. This window is based on the boundary of the horizontal region detected in the previous scan line. The analysis window for the first scan line is the entire line (the first scan line is assumed to be entirely in the road). In order to eliminate the effect of obstacles or ditches when measuring σ, we include only those points in the value range $\mu \pm k\mu$. Another technique to eliminate the effect of obstacles on the standard deviation of the *ith* scan line (σ_i) is to discard those points with value outside $\mu_i \pm k\sigma_{i-1}$ (based on the assumption that the noise level changes slowly). The following sections describe the use of μ and σ in detecting the horizontal region boundaries and finding obstacles in the region.

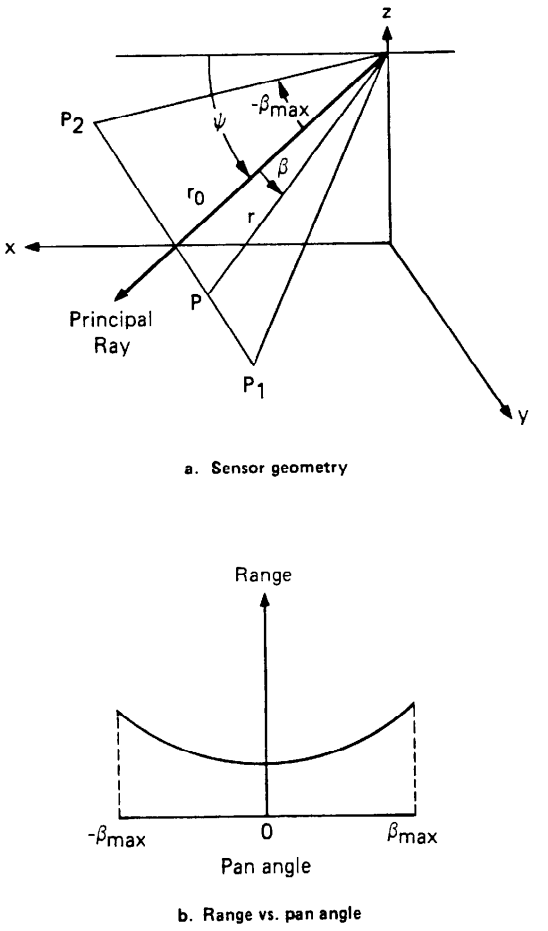

Figure 4: Scanning a Horizontal Plane

C. Detecting Horizontal Region Boundaries

Given μ_i and σ_i, we detect the left road-region boundary of the *ith* scan line by locating a sequence of range values that are within $\mu \pm k_1\sigma$. We start searching for this sequence at a point k_2 pixels outside (to the left of) the left boundary of the previous scan line. The parameter k_2 is currently set to zero because of perspective; we expect the apprarent road width to narrow slowly with increasing distance. The left boundary is the first point in the sequence. We limit the change in boundary position to a value based on the width of the road detected in the previous scan line in order to safeguard later processing from possible errors. Detecting the right boundary is similar.

An example of this processing is shown in Figure 5. The lower-left corner displays an ERIM image that has been corrected for ambiguity interval. The lower-right corner plots range values for several scan lines and illustrates the characteristic curvature of horizontal regions (compare to Figure 4b). Note the large change in range values along two scan lines that is caused by the presence of an obstacle. The upper right shows plots of range values after correcting for the pan angle. The location of the road boundaries are also marked in the upper right. The upper-left corner displays the detected road region. The arrow in the upper-left corner indicates the range image rows that contain the obstacle.

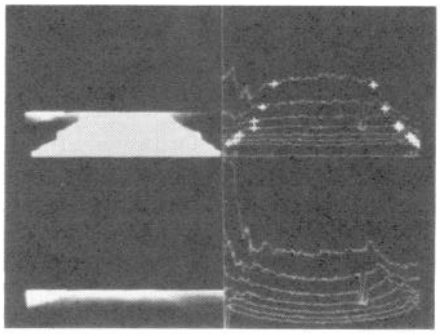

Figure 5: Detecting the Road Region

D. Detecting Jump Boundaries Using Sigma

After locating the left and right road boundaries and calculating μ and σ, we detect obstacles by finding horizontal and vertical discontinuities in range values (called jump boundaries) as specified below. The value $r_{i,j}$ is the range value for pixel j on scan line i.

- Smooth the range values between the left and right road boundaries using a 1 by 3 kernel.
- Detect a horizontal jump if $| r_{i,j} - r_{i,j+2} | > C_1\sigma_i$.
- Detect a vertical jump if $| r_{i,j} - r_{i-1,j} | > C_2\sigma_{i-1}$.

After detecting these jump boundary locations, we link them into larger units by a grow-and-shrink operation that connects jumps up to 4 pixels apart. Figure 6 shows an example of this method with the obstacle shown between the road boundaries in the upper-left corner.

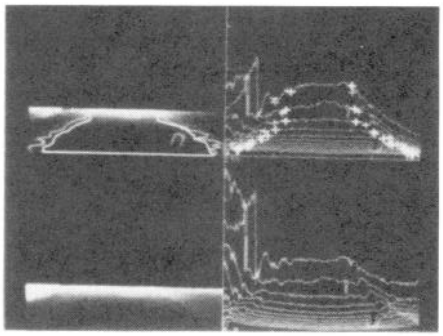

Figure 6: Detecting Jump Boundaries

We found that using σ to detect jump boundaries provides better results than other methods that we tested. Figure 7 shows jumps detected when

$$\frac{\Delta r}{r} > k \quad (r = \textit{range value}) \ .$$

This dynamic threshold method correctly locates distant obstacles and does not miss significant range discontinuities near the vehicle. However, this technique is adversely affected by the noise at the bottom of the image.

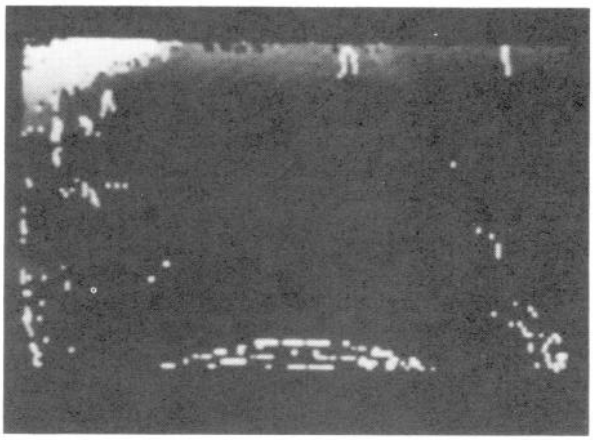

Figure 7: Jumps Detected with $\frac{\Delta r}{r} > k$

E. Finding Ditches and Shoulders

Roads often have shoulders and ditches that must be avoided (if large) and which may aid in navigation because they are usually parallel to the road. In order to locate these features, we examine a window outside the left and right road boundaries of each scan line, drawing a line between the road edge and the end of the window. The highest and lowest deviations from this line define the location of the shoulder and ditch respectively. In Figure 6, the ditches are shown as the outermost lines in the upper-left corner. The shoulders of the road are between the ditch and the road boundary.

The deviation in range data measured from a shoulder or ditch of constant height increases with distance from the ERIM scanner because the angle between the surface and the laser beam decreases (becomes more oblique) with distance (see Figure 8). As previously mentioned, the noise level also increases as the angle decreases, with the result that shoulders and ditches are detected most precisely at an intermediate distance--not too close or too far.

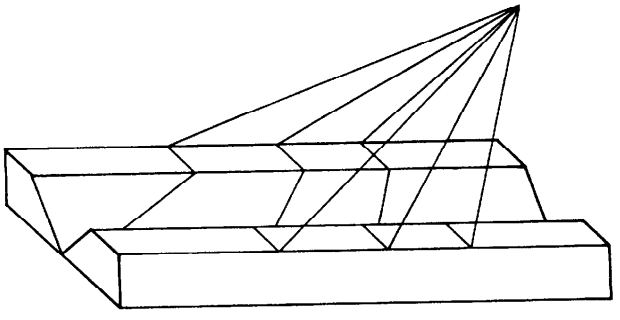

Figure 8: Scanning Configuration for a Ditch

F. Experimental Results

The methods described in the previous section were tested on five images--three of the type displayed in this paper and two range images of a park scene with trees. Good results were obtained on all the images without modifying the parameters k_1,k_2 or C_1,C_2. As an indication of the sensitivity of these techniques to choice of parameter value, we modified each parameter by 25% of its value and experienced no significant failures. For example, the value of k_1 controls the effect of range value deviations (e.g., obstacles) on the detected road boundary. The value of k_1 used in Figure 5 differs by 25% from the value used in Figure 6. It is possible to observe the effect of this change by closely examining the road width for the scan lines that contain the obstacle (indicated by the arrow in the upper left quadrant of each figure). In Figure 5 the obstacle causes a deviation in the detected road boundary. The detected road boundary in Figure 6 (indicated by the innermost pair of lines) is not greatly affected by the obstacle.

IV CONCLUSION

In this paper we presented new techniques for analyzing range images by measuring the noise level in each scan line. The mean and standard deviation of the noise are used as the basis for several adaptive thresholds. These methods process each scan line separately and are therefore quite fast. The techniques incorporate the measured noise level to detect horizontal regions and locate obstacles in the range data. Techniques to identify ditches and shoulders along the road were also presented.

REFERENCES

1. Binford, T.O., and J.M. Tenenbaum, "Computer Vison," *Computer*, Vol. 6 (May 1973).

2. Hebert, M., and T. Kanade, "First Results on Outdoor Scene Analysis Using Range Data," *Proc. of Image Understanding Workshop*, Miami, Florida (December 1985).

3. Nitzan, D., "Scene Analysis Using Range Data," 69, SRI International, Menlo Park, California (1972).

4. Nitzan, D., A.E. Brain, and R.O. Duda, "The Measurement and Use of Registered Reflectance and Range Data in Scene Analysis," *Proc. IEEE*, Vol. 65, No. 2 (February 1977).

5. Ross, M., *Laser Receivers*, John Wiley and Sons, New York, New York, 1966.